Journal of Power Sources 248 (2014) 190–195

Contents lists available at ScienceDirect

Journal of Power Sources

journal homepage: www.elsevier.com/locate/jpowsour

Short communication

Improvement of the redox durability of Ni-gadolinia doped ceria anodes due to the use of the composite particles prepared by spray pyrolysis method

Satoshi Hashigami*, Hiroyuki Yoshida, Daisuke Ueno, Mitsunobu Kawano, Toru Inagaki

The Kansai Electric Power Co., Inc., Energy Use R&D Center, 11-20 Nakoji 3-Chome, Amagasaki, Hyogo 661-0974, Japan

HIGHLIGHTS

- The NiO-GDC composite particles prepared by spray pyrolysis were used as an anode.
- The redox behaviors of Ni-GDC anodes were examined.
- The decrease of the cell voltage was small by using the composite particles.
- The composite particles suppressed the excessive agglomerations of nickel.

ARTICLE INFO

Article history:
Received 16 July 2013
Received in revised form
13 September 2013
Accepted 17 September 2013
Available online 25 September 2013

Keywords:
Spray pyrolysis
Ni-GDC
AC impedance
SEM
Solid oxide fuel cells

ABSTRACT

The redox behaviors of Ni-gadolinia doped ceria (GDC) anodes with different compositions and microstructures were investigated. When the NiO-GDC composite particles prepared by spray pyrolysis were used for an anode (SP-cells), the decrease of the cell voltage during the redox cycles was smaller than that of the cell with anode using the mixed powder of NiO and GDC (Mix-cells). Current interruption and AC impedance measurements were examined before redox cycle, after 1st redox cycle, and after 10th redox cycles. The ohmic and polarization losses after 10th cycles for SP-cells were smaller than those for Mix cells. The morphology changes of the Ni-GDC anodes between before-redox cycle and after-10th redox cycles were observed by scanning electron microscopy (SEM). These results indicate that the use of NiO-GDC composite particles suppressed the excessive agglomerations of nickel grains during the redox cycles.

1. Introduction

Ceria-based anodes have been proposed as anode materials for solid oxide fuel cells (SOFCs) [1]. Among them, gadolinia-doped ceria (GDC) is considered to be one of the promising candidates because of high ionic and electronic conductivities in reducing atmosphere. Therefore, cermet of Ni and GDC has been usually used as an anode for SOFCs.

Even though nickel in the anode remains in reduced state during normal operation, reoxidation of the anode may occur by accidents, such as the interruption of fuel supply and the incorporation of air into anode side. Consequently, structure destruction of the anode and deterioration of the performance during redox cycles may occur. Furthermore, some researchers reported that redox cycles caused a change of anode volume and lowered cell performances [2,3]. Thus, it is demanded to develop electrodes giving high redox durability.

We have reported that the anode fabricated from the composite particles synthesized by spray pyrolysis showed higher electrochemical activity than that fabricated from the mixture of NiO and doped ceria particles [4]. In addition, the microstructure of the composite particles has been investigated by X-ray diffraction, X-ray absorption fine structure, scanning electron microscope, and transmission electron microscope and energy-dispersive X-ray spectroscopy [5]. In the previous study, we reported cerium in NiO-doped ceria composite particles synthesized by spray pyrolysis was concentrated at around the surface of the particles, and nickel existed all over inside the particles [4]. This kind of internal structure was considered to prevent over-agglomeration during sintering of the anode and to form the optimal anode structure.

From these results, the anode fabricated from the composite particles is expected to give higher durability for redox cycles as

* Corresponding author. Tel.: +81 50 7104 2640; fax: +81 66 494 9709.
E-mail address: hashigami.satoshi@c5.kepco.co.jp (S. Hashigami).

0378-7753/$ – see front matter © 2013 Elsevier B.V. All rights reserved.
http://dx.doi.org/10.1016/j.jpowsour.2013.09.073

well as initial performance. In this study, the changes of electrochemical performances and microstructures of the anode fabricated from the composite particles were investigated during the redox cycles, and were compared with those fabricated from mixed powder of NiO and GDC.

2. Experimental

2.1. Preparation of the NiO-GDC composite particles

The NiO-GDC composite particles were synthesized by using spray pyrolysis apparatus as shown in Fig. 1.

0.09 mol of cerium nitrate hexahydrate and the corresponding amounts of gadolinium nitrate hexahydrate and nickel-acetate tetrahydrate were mixed into 500 ml of deionized water, and added 120 ml of concentrated nitric acid, and stirred for an hour. Finally, deionized water was added to be 1 L aqueous solution and used as starting solution. The atomic ratio of Ce:Gd was set to 9:1 and the atomic ratio of Ni and Ce was determined so that the weight ratio of NiO:GDC should be 7:3 or 8:2. The reaction furnace consisted of four independent heating zones, whose temperatures were set at 200, 400, 800, and 1000 °C, respectively. Starting solution was atomized by ultrasonic vibrators, and formed mists were flown into the furnace with 1 L min^{-1} of air. For comparison, the mixture of NiO and GDC powders was also prepared as anode material. Ce/Gd and Ni/Ce ratios in NiO-GDC mixtures were set to the same values as those of composite particles.

2.2. Cell fabrication and testing conditions

NiO-GDC powder was screen-printed onto the electrolyte ($La_{0.9}Sr_{0.1}Ga_{0.8}Mg_{0.2}O_{3-\delta}$:LSGM, 32 mm in diameter and 0.2 mm in thickness) and fired in air at 1200 °C or 1280 °C. The sintering temperature range was adapted on the basis of the results we obtained in our previous works, in which sintering the composite particles on to LSGM disks at 1200–1300 °C gave the highest anode performance [6,7]. Screen-printing of $Sm_{0.5}Sr_{0.5}CoO_3$(SSC) cathode onto the opposite side of electrolyte and firing at 1100 °C (electrode diameter was set to 16 mm) are performed. Table 1 shows the list of samples tested in this study. Samples were named after preparation method of anode materials, NiO ratio in anode by weight, and firing temperature of the anode. For example, the cells with anode fabricated from the powder prepared by spray pyrolysis with NiO ratio of 70 wt% fired at 1200 °C were denoted as SP-70-1200.

Each fabricated cell was installed on a testing apparatus and heated to 750 °C with N_2 gas supplied to both the anode and the cathode sides. After the temperature was stabilized at 750 °C, NiO in the anode was reduced by dry H_2 gas (100 ml min^{-1}). Air (100 ml min^{-1}) was introduced to the cathode side instead of N_2. The initial cell performance was investigated and then the redox cycle test was examined. The redox cycle test of the anode was examined as follows. (i) The reduced anode was oxidized by Air for 10 min at 100 ml min^{-1}. (ii) The oxidized anode was reduced by H_2 for 20 min at 100 ml min^{-1}. Steps (i) and (ii) were repeated. N_2 was used to purge the anode atmosphere between each step.

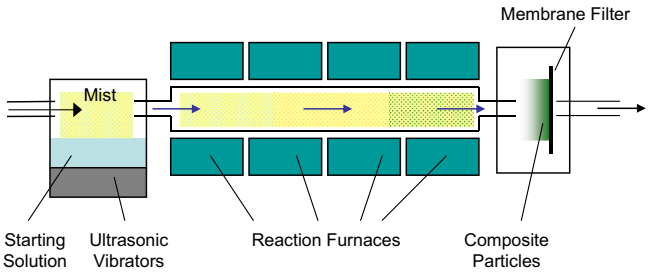

Fig. 1. Schematic illustration of spray pyrolysis apparatus.

Table 1
List of the cell samples with Ni-GDC anode investigated in this study.

Sample name	Anode synthesis method	NiO amount in anode/wt%	Firing temperature of anode/°C
Mix-70-1200	Powder mixing	70	1200
Mix-70-1280	Powder mixing	70	1280
SP-70-1200	Spray pyrolysis	70	1200
SP-70-1280	Spray pyrolysis	70	1280
SP-80-1200	Spray pyrolysis	80	1200
SP-80-1280	Spray pyrolysis	80	1280

Current interruption and AC impedance measurements (frequency sweep between 1 MHz and 0.1 Hz) were examined prior to the redox cycle test, after 1st redox cycle, and after 10th redox cycles. Dividing the cell voltage loss into ohmic loss and overpotential loss was carried out for each method. The morphology changes of the Ni-GDC anodes between before-redox cycle and after-10th redox cycles were observed by scanning electron microscopy (SEM). The SEM samples were in the reduced state since the cells were tested after 10th redox cycles in H_2 flow and lower the temperature in N_2 flow.

3. Results and discussion

3.1. Cell voltage change during redox cycles

The change of the cell voltage after each redox cycle at the current density of 0.3 A cm^{-2} was shown in Fig. 2. The cell voltages after the first redox cycle were increased from the initial state for all cells, especially, in the case of SP-70-1200, noticeable cell voltage increase was observed. This kind of behavior has been previously reported [8,9]. It is considered that the network structure formation of nickel was insufficient by firing of anode at 1200 °C and was progressed during 1st redox cycle to increase electrical paths.

In the case of Mix-70-1200, initial cell performance was relatively high, however, the decrease of the cell voltage during the redox cycles was large. On the other hand, redox durability of Mix-

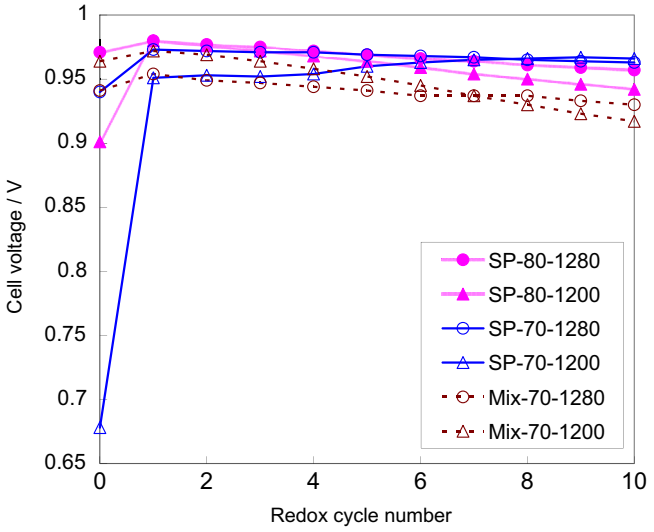

Fig. 2. The variations of the cell voltages for Ni-GDC|LSGM|SSC cells at 750 °C with the current density of 0.3 A cm^{-2} depending on the number of times of redox cycles.

70-1280 was better than Mix-70-1200. Therefore, initial cell performance and durability during the redox cycles are related to trade-off in the case of Mix cells. In the case of SP cells, the cell voltages after 10th redox cycles were almost the same or higher than those before redox cycle. Judged from these results, the decrease of the cell voltage during the redox cycles was considered to be affected by microstructures of anode materials.

The influence of NiO/GDC ratio of the anode materials given to the durability for redox cycles was also investigated. The increase of NiO/GDC ratio for SP cells gave the improvement of initial cell performance regardless of the firing temperature, however, the decrease of the cell voltage occurred during 10 redox cycles. These results indicate that higher NiO/GDC ratios promote the agglomerating and sintering of nickel during the redox cycles. We also tried to fabricate Mix-80 cells for comparison, however, anodes were delaminated after firing due to the difference of thermal expansion coefficient between NiO and LSGM electrolyte substrate. In the case of SP cells, NiO was covered with GDC, and the thermal expansion coefficient of GDC and LSGM is almost the same, therefore, the anode could be fabricated with relatively high NiO/GDC ratio.

3.2. Dividing the voltage drops into the ohmic and the overpotential losses

The ohmic loss and the overpotential loss of each cell measured by current interruption methods during the redox cycles at 750 °C were shown in Fig. 3. The ohmic loss was significantly large for SP-70-1200 before redox cycle. This result indicated that nickel in the composite particles prepared by spray pyrolysis was covered with GDC and the network formation of nickel was insufficient after firing at 1200 °C. Ohmic and overpotential losses were decreased during 1st redox cycle in all samples, which was considered that the active triple phase boundary (TPB) length and the electrical path were increased by the growth of the network structure of nickel and GDC. Pihlatie et al. reported a 60% reduction in the total polarization resistance after redox cycle [9] and Young et al. showed that the anode conductivity with redox cycling increased [10].

For SP-70-1200 and SP-70-1280, additional decrease of the ohmic and overpotential losses was observed during the redox cycles, while they increased for the other samples. The resistance increase was considered to come from the deformation of nickel network structure, the delamination between electrolyte and electrode, and the decrease in electrochemical activity as a consequence of decreased active TPB length. For SP-70-1200 and SP-70-1280, it was indicated that the use of the composite particles suppressed the excessive agglomerations of nickel grains during the redox cycles, while the agglomerations of nickel significantly progressed for the others. In the case of SP cells, the ohmic loss before redox cycle was drastically decreased by increasing the nickel content, which brought the expansion of nickel network and the improvement of the electrical conductivity. On the other hand, the increasing of the nickel ratio in the anode led to the increasing of the overpotential loss since the TPB length decreased by the agglomeration of nickel.

To analyze the overpotential loss in detail, AC impedance measurements were examined. The impedance spectra at initial state and after 1st and 10th redox cycles were shown in Fig. 4. A distorted semicircle and a short straight line having an angle of 45° with the real axis were observed on each spectrum. Higher frequency (left side) intercept of a semicircle with the horizontal axis was ascribed to the ohmic resistance of the cell (R_i). A semicircle represents resistance of electrochemical reactions on the electrodes (R_p), and a straight line (a Warburg-like response) represents diffusion resistance. Although the impedance spectra include the impedances of cathode side, it should not be changed during anode redox cycles, therefore, the change of impedance spectra can be regarded as the change of anode.

In the case of Mix cells (Fig. 4(a), (b)) and SP-80 cells (Fig. 4(e), (f)), R_ps after 10th redox cycles became larger than that after 1st redox cycle. On the other hand, for SP-70 cells (Fig. 4(c), (d)), the increase of R_ps during redox cycles were not apparent. It is considered that the increase and decrease of TPB length is related. R_is after 10th redox cycles were larger compared with that after 1st redox cycle in the case of Mix cells (Fig. 4(a), (b)) and SP-80 cells (Fig. 4(e), (f)). For SP-70 cells (Fig. 4(c), (d)), however, R_is during redox cycles were decreased. It is related to the growth of electrical paths. These behaviors of R_i and R_p were in consistent with the results of current interruption methods (Fig. 3). The slopes of the lines of impedance spectra did not change during redox cycles, which confirmed that the deterioration of cell performance during redox cycles was due to the variation of the electrical conductivity and the electrochemical activity rather than the deterioration of gas

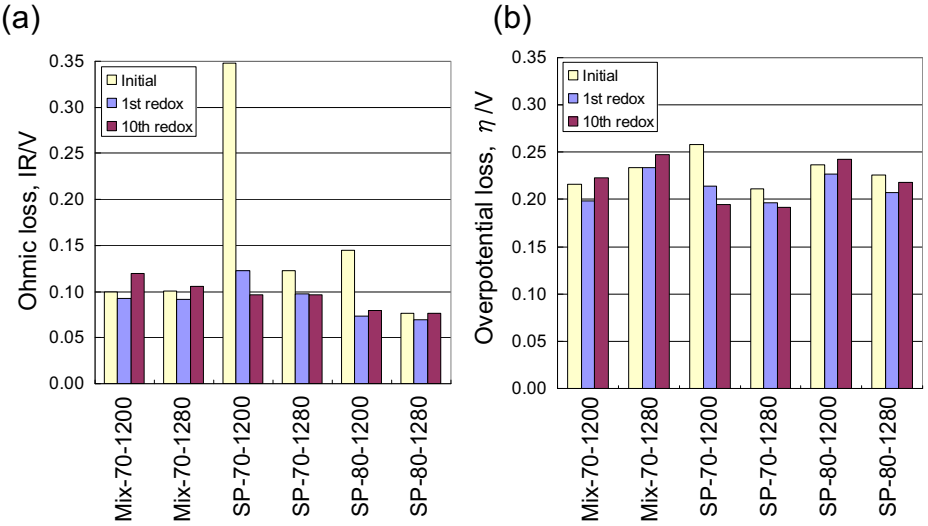

Fig. 3. The variations of ohmic and overpotential losses during redox cycles at 750 °C with the current density of 0.3 A cm^{-2} measured by current interruption method ((a): ohmic loss (b): overpotential loss).

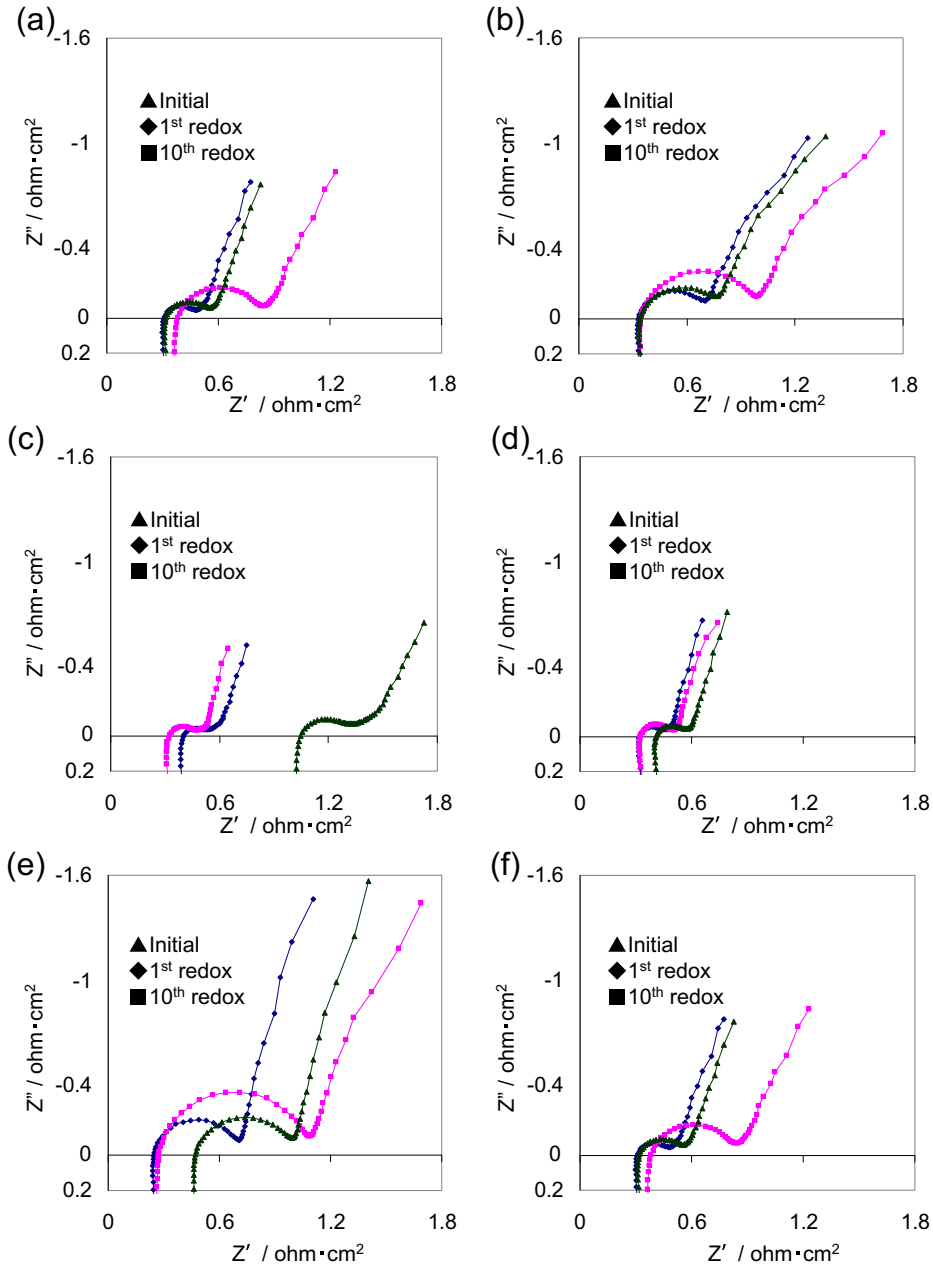

Fig. 4. Impedance spectra for Ni-GDC|LSGM|SSC cells at 750 °C under open-circuit conditions depending on the number of times of redox cycles ((a): Mix-70-1200 (b): Mix-70-1280 (c): SP-70-1200 (d): SP-70-1280 (e): SP-80-1200 (f): SP-80–1280).

diffusion property. Therefore, microstructures of the anodes before and after redox cycles were observed by SEM.

3.3. Microstructure observation by SEM

The SEM images of Ni-GDC anode surface at the initial state and after 10th redox cycles are shown in Figs. 5–7. The original core–shell structures of the NiO-GDC composite particles were collapsed and the network structures of the anodes were formed depending on the sintering temperature [11]. Therefore, the electrode microstructures observed by SEM compares the state of the network structures. Dark gray region is ascribed to Ni, light gray is to GDC, and black is to pores. Distribution of each component was confirmed by energy dispersive X-ray spectroscopy (EDS). For Mix cells (shown in Fig. 5), the agglomerations of Ni occurred during 10 redox cycles regardless of firing temperatures. In the case of SP-70 cells (shown in Fig. 6), any excessive coarsening of nickel was not observed, which was consistent with the steady cell voltage during redox cycles (Fig. 2). It is considered to be related to the fact that cerium was concentrated at around the surface of the particles, and that nickel existed all over inside the particles [4]. In the case of SP-70-1280 cell (Fig. 6(c)), the spherical shape was partially collapsed. On the other hand, the spherical shape of SP-70-1200 cell (Fig. 6(a)) remained. These results indicated the growth of network structure of nickel by increasing sintering temperature.

Fig. 7 shows the SEM images of the anode in SP-80 cells before and after redox cycles. In the case of SP-80-1280 (Fig. 7(c), (d)), there is no change for microstructure before and after 10th redox cycles, which relates to the result that the initial cell performance is

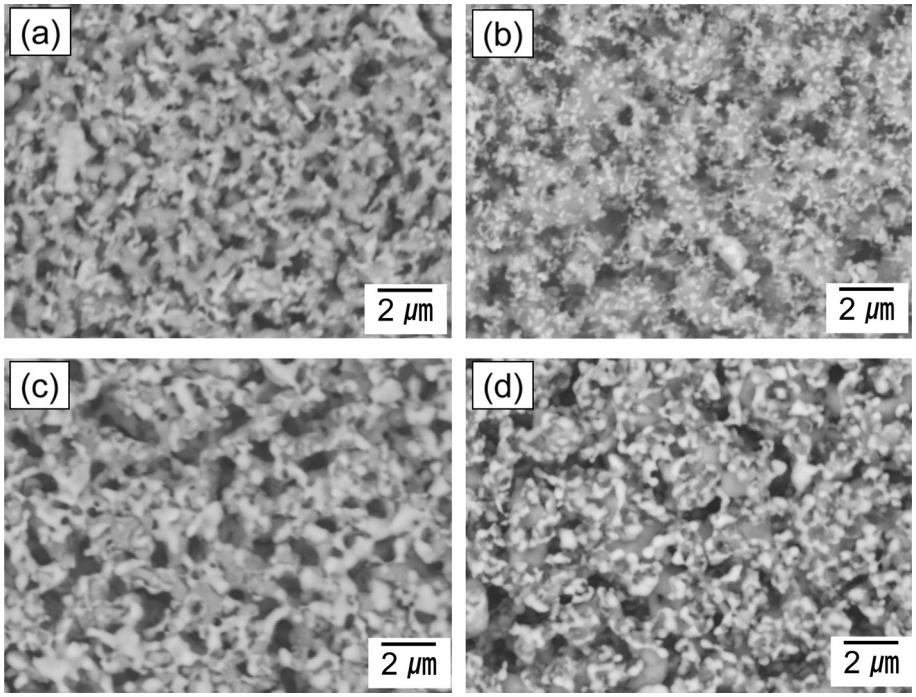

Fig. 5. SEM images of Ni-GDC anode surface fabricated from mixed powder ((a): Mix-70-1200-initial state (b): Mix-70-1200-after 10th redox cycle (c): Mix-70-1280-initial state (d): Mix-70-1280-after 10th redox cycle).

almost the same as the cell performance after 10th redox cycles (Fig. 2 (SP-80-1280)). As shown in Fig. 7(b), the agglomeration of ceria occurred in SP-80-1200 after 10th redox cycle compared with SP-80-1280 after 10th redox cycle (Fig. 7(d)). It may be attributed to fine distribution of ceria in the anode that the cell voltage was relatively maintained during the redox cycles for SP-80-1280 (Fig. 2). The original spherical shape before redox cycle was almost not observed (Fig. 7(b)) and it may lead excessive coarsening of nickel and the deterioration of cell performance following redox cycles for SP-80-1200 (Fig. 2). From these results, in the case of the NiO-GDC composite particles prepared by spray pyrolysis, the optimum NiO ratio in NiO-GDC and sintering temperature are suggested to be the range between 70 and 80 wt% and between 1200 and 1280 °C, respectively.

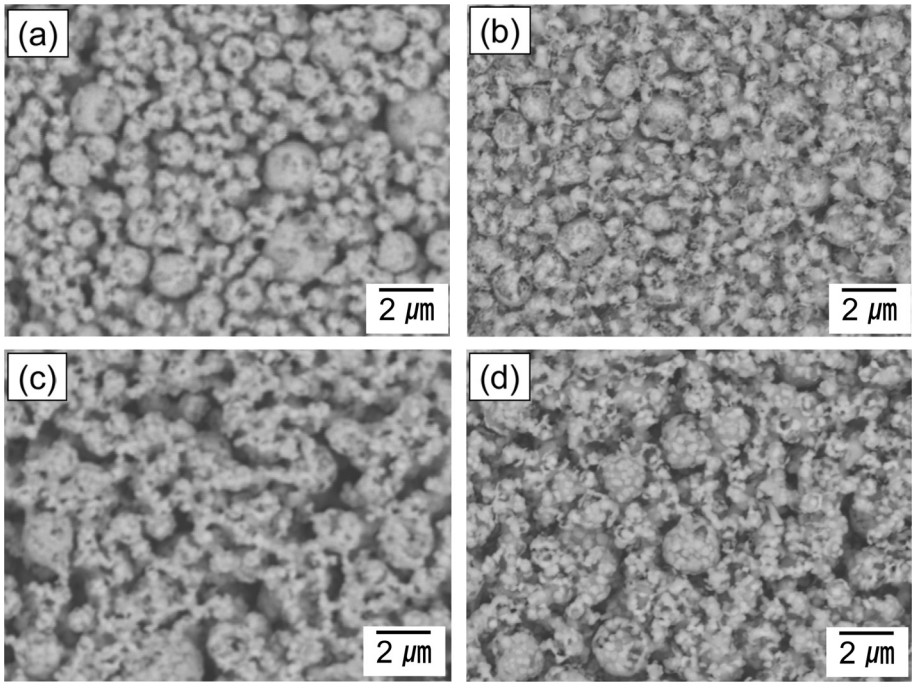

Fig. 6. SEM images of Ni-GDC anode surface fabricated from composite particles ((a): SP-70-1200-initial state (b): SP-70-1200-after 10th redox cycle (c): SP-70-1280-initial state (d): SP-70-1280-after 10th redox cycle).

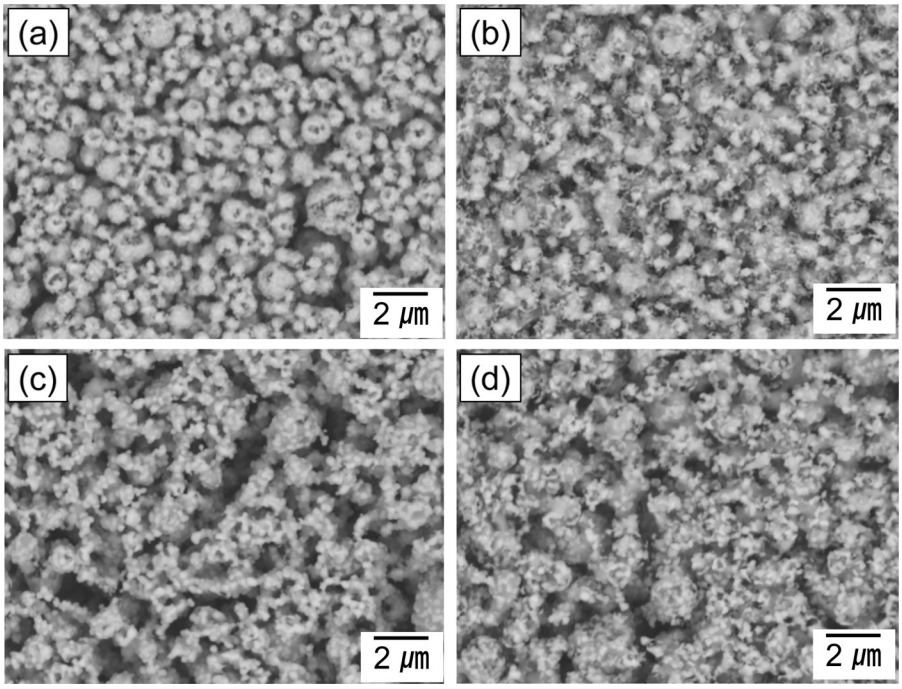

Fig. 7. SEM images of Ni-GDC anode surface fabricated from composite particles ((a): SP-80-1200-initial state (b): SP-80-1200-after 10th redox cycle (c): SP-80-1280-initial state (d): SP-80-1280-after 10th redox cycle).

4. Conclusions

The redox behaviors of Ni-GDC anodes with different compositions and microstructures were investigated. When the NiO-GDC composite particles prepared by spray pyrolysis were used for an anode, the decrease of the cell voltage during the redox cycles was smaller than the cell with the anode using the mixed powder of NiO and GDC at the same NiO/GDC ratio. The current interruption methods showed that the increase of ohmic loss and overpotential loss during the redox cycles was smaller for SP cells than that for Mix cells. The composite particles used in this study had core–shell structure in which NiO was covered with GDC, and it was considered that the use for the composite particles suppressed the excessive agglomerations of nickel grains during the redox cycles. The increase of NiO/GDC ratio gave the improvement of initial cell performance, however, it caused the decrease of the cell voltage during 10 redox cycles. This result indicates excessively high NiO/GDC ratios promote the agglomerating and sintering of nickel during the redox cycles.

References

[1] M. Mogensen, T. Lindegaard, U.R. Hansen, in: Proceedings of the Second International Symposium on Ionic and Mixed Conducting Ceramics, 1994, pp. 448–465.
[2] Y. Zhang, B. Liu, B. Tu, Y. Dong, M. Cheng, Solid State Ionics 180 (2009) 1580–1586.
[3] A. Faes, Z. Wuillemin, P. Tanasini, N. Accardo, J. Van Herle, J. Power Sources 196 (2011) 3553–3558.
[4] S. Suda, M. Itagaki, E. Node, S. Takahashi, M. Kawano, H. Yoshida, Toru Inagaki, J. Eur. Ceram. Soc. 26 (2006) 593–597.
[5] H. Yoshida, H. Deguchi, M. Kawano, K. Hashino, T. Inagaki, H. Ijichi, M. Horiuchi, K. Kawahara, S. Suda, Solid State Ionics 178 (2007) 399–405.
[6] R. Maric, S. Ohara, T. Fukui, T. Inagaki, J. Fujita, Electrochemical Solid-State Lett. 1 (5) (1998) 201–203.
[7] Xinge Zhang, S. Ohara, R. Maric, K. Mukai, T. Fukui, H. Yoshida, M. Nishimura, T. Inagaki, K. Miura, J. Power Sources 83 (1999) 170–177.
[8] T. Hatae, Y. Matsuzaki, S. Yamashita, Y. Yamazaki, J. Electrochem. Soc. 157 (2010) B650–B654.
[9] M. Pihlatie, T. Ramos, A. Kaiser, J. Power Sources 193 (2009) 322–330.
[10] J.L. Young, V. Vedahara, S. Kung, S. Xia, V.I. Briss, ECS Trans. 7 (1) (2007) 1511–1519.
[11] H. Yoshida, M. Kawano, K. Hashino, T. Inagaki, in: 7th Asian Conference on Electrochemistry, 2010, p. 125.